Arabian Journal of Chemistry (2021) **14**, 103201

King Saud University

Arabian Journal of Chemistry

www.ksu.edu.sa
www.sciencedirect.com

ORIGINAL ARTICLE

Decorated CuO nanoparticles over chitosan-functionalized magnetic nanoparticles: Investigation of its anti-colon carcinoma and anti-gastric cancer effects

Yuping Wang [a], Attalla F. El-Kott [b,c], Ayman E. El-Kenawy [d], Liangjun Xue [e,*]

[a] *Department of Oncology Wards 1, Henan Province Hospital of TCM (The Second Affiliated Hospital of Henan University of Chinese Medicine), Zhengzhou City, Henan Province 450000, China*
[b] *Biology Department, College of Science, King Khalid University, Abha 61413, Saudi Arabia*
[c] *Zoology Department, College of Science, Damanhour University, Damanhour 22511, Egypt*
[d] *Pathology Department, College of Medicine, Taif University, Taif 11099, Saudi Arabia*
[e] *Department of Radiotherapy, Yijishan Hospital of Wannan Medical College, Wuhu 241001, China*

Received 18 February 2021; accepted 2 May 2021
Available online 24 May 2021

KEYWORDS

Copper oxide;
Chitosan;
Magnetic nanocomposite;
Gastric cancer;
Colorectal carcinoma

Abstract In this study, a green protocol for supporting CuO nanoparticles over chitosan-modified amino-magnetic nanoparticles is described. The physicochemical and morphological properties of the desired nanocomposite assessed by various techniques like ICP, FT-IR, FE-SEM, EDX, TEM, XRD and VSM. In the oncological part of the recent study, the $Cu(NO_3)_2$, Fe_3O_4, and Fe_3O_4-NH_2@CS/CuO nanocomposite cell viability was very low against human gastric cancer cell lines i.e. MKN45, AGS, and KATO III and human colorectal carcinoma cell lines i.e. HT-29, HCT 116, HCT-8 [HRT-18], and Ramos.2G6.4C10. The IC50 of Fe_3O_4-NH_2@CS/CuO nanocomposite against MKN45, AGS, KATO III, HT-29, HCT 116, HCT-8 [HRT-18], and Ramos.2G6.4C10 cell lines were 517, 525, 544, 282, 214, 420, and 477 μg/mL, respectively. Thereby, the best anti-gastro-duodenal cancers findings of our Fe_3O_4-NH_2@CS/CuO nanocomposite was seen in the HCT 116 cell line case.

1. Introduction

The gastro-duodenal system is one of the main systems of the body that has been distributed from the mouth to anus and digest and absorb the nutritional materials in the food. The major illnesses that affect the usual action of the gastro-duodenal tract are ulcerative colitis, tapeworms, stomach

* Corresponding author.
E-mail address: xuelj016@sina.com (L. Xue).
Peer review under responsibility of King Saud University.

ELSEVIER Production and hosting by Elsevier

https://doi.org/10.1016/j.arabjc.2021.103201
1878-5352 © 2021 Published by Elsevier B.V. on behalf of King Saud University.

ulcers, listeria infection, celiac disease, gallstones, acid reflux (GERD), appendicitis, lactose intolerance, inflammatory bowel disease, and gastro-duodenal cancers. In this regard, the gastro-duodenal cancers mortality rate is high (Astin et al., 2011). The risk factors are polyp's personal history, obesity, smoking, high-fat diet, inherited syndromes, radiation therapy, diabetes, older age, sedentary lifestyle, gastro-duodenal cancers family history, and alcohol (Astin et al., 2011; Juul et al., 2018; Lauby-Secretan et al., 2016; Cunningham et al., 2010). The gastro-duodenal cancers signs are weight loss, anemia or rectal bleeding, decrease in stool caliber, vomiting or nausea, worsening constipation, and loss of appetite (Astin et al., 2011; Juul et al., 2018). Several chemotherapeutic supplements/drugs including oxaliplatin, irinotecan, cetuximab, panitumumab, and fluorouracil can be administrated to treat human gastro-duodenal cancers in the patients (Shaib et al., 2013). Chemotherapeutic supplements have severe side effects for the patients, so finding modern formulations with low side effects are the priority of the Food and Drug Administration. The previous reports have revealed the metallic nanocomposites have unique anticancer efficacies with low side effects (Shaib et al., 2013; Raut et al., 2010).

Today, nanoparticles have become very popular due to their wide applications in biology, medicine and medicine. Structurally, their size is in the range of 100 nm. In general, there are various physical and chemical methods ultraviolet and microwave radiation and laser for the synthesis of metallic nanoparticles. Chemical methods do not work well due to the production of toxic chemical compounds and compared to other methods, environmentally friendly bio-methods are preferred for the synthesis of metallic nanoparticles, as these methods are single-step and do not require reducing and stabilizing compounds (Raut et al., 2010). Biological methods are suitable options for the synthesis of metallic nanoparticles so that the rate of metallic ion reduction is very high. Biological methods are low cost and high yield and lead to the production of nanoparticle crystal structures of different sizes and this depends on the nature of the plant extract, pH, temperature and incubation time (Shaib et al., 2013; Raut et al., 2010). A wide range of medial supplements such as small hydrophilic and hydrophobic vaccines, drugs, and molecules of biological nanoparticles may be administered by the metallic nanoparticles. They are widely used in improving the treatment and diagnosis of diseases. Nanoparticles in the form of nanofibers, carbon nanotubes, nanoliposomes, nanospheres widely have been administrated for cell scaffolding and drug carriers. Applications of nanoparticles in drug delivery include drug carriers in disorders such as tumor, cardiovascular disease, Alzheimer's. The use of these nanocarriers is very effective for neurological diseases such as Alzheimer's because these nanoparticles can cross the blood–brain barrier due to their size that this barrier has always been a barrier to the passage of drugs to the affected area in this type of destructive brain disease (Raut et al., 2010). Due to the metallic nanoparticles low size, they can also be used in brain cancers. The main aim in making metallic nanoparticles is to control the surface properties, particle size, and release of a specific and efficient drug in a specific place and time for the drug to be as effective as possible (Shaib et al., 2013). Nanoparticles have many therapeutic applications and have always been used to treat various diseases. Their use in the cure of infectious, fungal, bacterial, viral, cutaneous, cardiovascular diseases and especially several cancers such as gastro-duodenal cancers has been amazing (Shaib et al., 2013; Raut et al., 2010; Lotfi and Veisi, 2019).

In this work, we wish to design and preparation of novel CuO NPs supported chitosan functionalized-magnetite nanoparticles (Fe_3O_4-NH_2@CS/CuO) for first time. The chitosan modified surface can easily have capped the Cu ions and stabilized CuO NPs (Scheme 1). Next, we determined the properties of Fe_3O_4-NH_2@CS/CuO nanocomposite in the cytotoxicity studies against human gastric cancer cell lines.

2. Experimental

2.1. Preparation of aminopropyl silica-coated Fe_3O_4 NPs (Fe_3O_4-NH_2)

Magnetic nanoparticles were prepared via co-precipitation of Fe (III) and Fe (II) ions with a molar ratio of 2:1 in the presence of ammonium hydroxide. Generally, a mixture of $FeCl_3{\cdot}6H_2O$ (5.838 g, 0.0216 mol) and $FeCl_2{\cdot}4H_2O$ (2.147 g, 0.0108 mol) was dissolved in 100 mL deionized water at 85 °C under N_2 atmosphere and intense mechanical stirring (500 rpm). Afterwards, 10 mL of 25% NH_4OH was quickly injected into the reaction mixture in one section. The addition of the base to the Fe^{2+}/Fe^{3+} salt solution resulted in the formation of the black precipitate of MNPs instantly. The reaction continued for another 25 min and the mixture was cooled to room temperature. The magnetic nanoparticles as a dark solid were isolated from the solution by magnetic separation and washed several times by DI water.

1.0 gm Fe_3O_4 NPs were added in 50 mL toluene and sonicated ure for 20 min and stirred for 30 min. Then, 0.1 mL 3-aminopropyl trimethoxysilane (APTMS) was then injected to the resulting mixture using a microsyringe and stirred continued for 1 h prior to the injection of (0.1 mL) and finish the surface modification with aminopropyl group. The obtained hybrid material (Fe_3O_4-NH_2) was collected with an external magnet and washed with ethanol and deionized water for three times and dried at 60 °C.

2.2. Preparation of Fe_3O_4-NH_2@CS/CuO nanocomposite

In a typical process, Fe_3O_4-NH_2 particles (0.5 g) were dispersed in 50 mL deionized water. A 30 mL homogeneous mixture of chitosan (0.2 g CS in 50 mL 1% HOAc) was added to the mixture. The resulted mixture was stirred and subsequently a glutaraldehyde aqueous solution (5 wt%, 10 mL) was added and stirred again 60 min at 50 °C. The resulted Fe_3O_4-NH_2@CS was collected by an external magnet, washed with ethanol and dried at 60 °C. Finally, 0.5 gm of Fe_3O_4-NH_2@CS composite was dispersed in 100 mL H_2O and sonicated for 20 min. Subsequently, an aqueous solution of Cu $(NO_3)_2$ (0.2 mmol in 20 mL H_2O) was added to reaction mixture and stirred for 12 h at room temperature. The Fe_3O_4-NH_2@CS/Cu^{2+} precursors were then hydrothermally (100 °C for 12 hrs) reacted using basic solution (NaOH, 0.5 mol/L), in order to grow CuO nanocrystals in the cross-linked chitosan matrix. The Fe_3O_4-NH_2@CS/CuO nanocomposite was collected using an external magnet and washed with distilled water and dried at ambient temperature. The Cu load was 0.28 mmol/g which measured by ICP-OES.

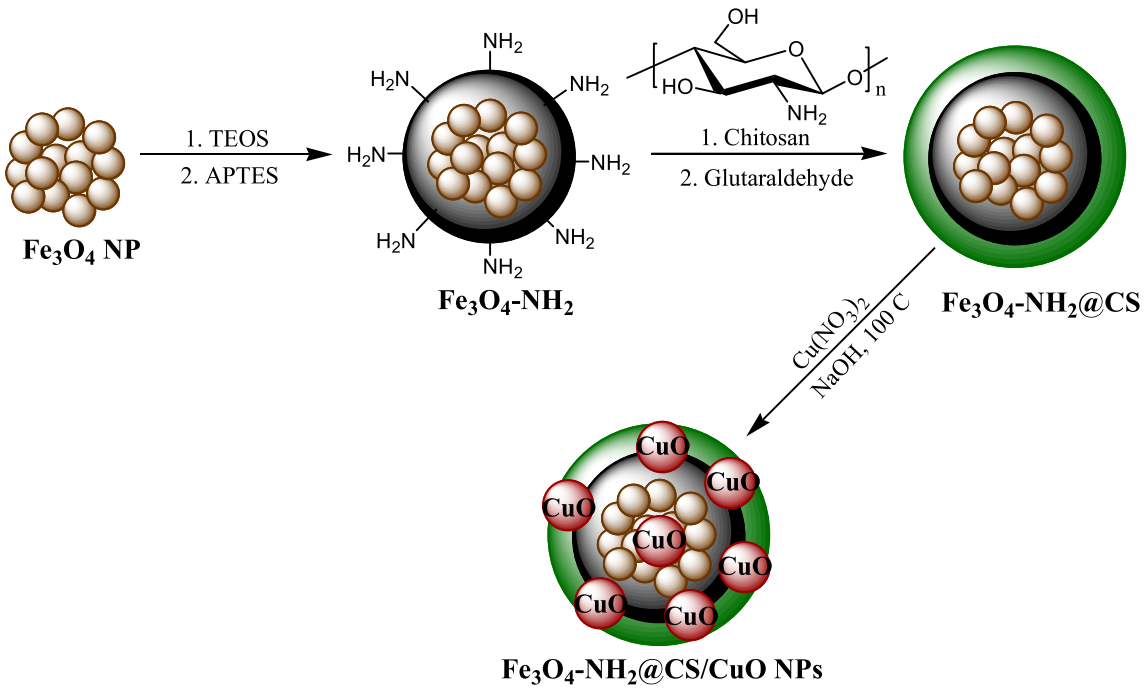

Scheme 1 Preparation of Fe_3O_4-NH_2@CS/CuO magnetic nanocomposite.

2.3. Determination of anti-human gastro-duodenal cancers potentials of Fe_3O_4-NH_2@CS/CuO nanocomposite by MTT assay

The MTT assay is a procedure of colorimetric based on reducing and breaking of yellow tetrazolium crystals by the enzyme succinate dehydrogenase to form insoluble purple crystals. In this method, unlike other methods, the steps of washing and collecting cells, which often cause the loss of a number of cells and increase the work error, have been eliminated and all test steps from the beginning of cell culture to reading the results with a photometer are performed on a microplate, so the repeatability, accuracy and sensitivity of the test are high (Shaib et al., 2013; Raut et al., 2010). If the test is performed on cells attached to the plate, an appropriate number of cells (about 2000 cells) must first be cultured in each of the wells. Then we select the control and test wells and add the appropriate amount of mitogen or drug to the test wells and place the plate in the incubator for the required time so that the desired substance affects the cells (Raut et al., 2010; Lotfi and Veisi, 2019). At the end of the incubation time, discard the supernatant and add 200 µl of culture medium containing half an mg/ml of MTT solution to each well and put it again in a carbon dioxide incubator for 2–4 h at 37 °C. During incubation, MTT is regenerated by one of the enzymes of the mitochondrial respiratory cycle i.e., succinate dehydrogenase. The regeneration and breakage of this ring produce purple-blue crystals of formazan that are easily detectable under a microscope. At the end, the optical absorption of the resulting solution can be read at 570 nm and the cells number can be calculated using a standard curve. For each cell line, there is a linear relationship between the number of cells and the light absorption of the final solution. Therefore, to examine each cell type, a standard curve related to the same cell line must be drawn and used (Raut et al., 2010; Lotfi and Veisi, 2019; Lu et al., 2021).

In this experiment, following human normal and gastro-duodenal cancers cell lines were used to determine the anti-cancer and cytotoxicity activity of gastro-duodenal over the $Cu(NO_3)_2$, Fe_3O_4, and Fe_3O_4-NH_2@CS/CuO nanocomposite using MTT assay:

(A) Human gastric cancer cell lines:
  (a) KATO III
  (b) AGS
  (c) MKN45

(B) Human colorectal carcinoma cell lines:
  (a) Ramos.2G6.4C10
  (b) HCT-8 [HRT-18]
  (c) HCT 116
  (d) HT-29

The cells were in RPMI1640 liquid culture medium containing 2 mM glutamine, 10% inactivated bovine fetal serum (FBS), solution of streptomycin (100 µg/ml) and penicillin (100 units per ml) at 37 °C and 5% CO_2 and 95% moisture were cultured and passaged so that the cells reached the desired number in terms of morphology and number (after 3–4 passages). After separating the cells from the flask surface, trypsin-EDTA (Gibco BRL, Scotland) counted and evaluated cell viability, and 3000 cells were cultured in 96-well wells without or with Fe_3O_4, $Cu(NO_3)_2$, and Fe_3O_4-NH_2@CS/CuO nanocomposite. Morphological changes and general characteristics of the cell were assessed 24 h using an inverted microscope (Motic, AE31 model, China) (Lu et al., 2021).

The effect of cytotoxicity of the Fe_3O_4, $Cu(NO_3)_2$, and Fe_3O_4-NH_2@CS/CuO nanocomposite was evaluated by

MTT Methy Thiazol Tetrazolium colorimetric test. MTT (Sigma-Aldrich, USA) is a tetrazolium salt based on living cell mitochondrial dehydrogenase succinate enzyme, which converts the yellow solution of MTT to insoluble purple crystals of formazan that is soluble in dimethyl sulfoxide (Lu et al., 2021).

The cells began to grow in 75 cm square T-flasks in 15 mL of medium with 10^6 cells initial number. After 72 h and covering the bottom of the flask with cell, the cell layer adhering to the bottom of the flask was separated enzymatically using trypsin-Versen and transferred to a sterile test tube was centrifuged at 1200 rpm for 10 min (Germany). Sigma, 3–30 k model). The cells were then resuspended in a new culture medium with a pasteurizer pipette and 100 µl of cell suspension without or with Fe_3O_4, $Cu(NO_3)_2$, and Fe_3O_4-NH_2@CS/CuO nanocomposite was added to each well of the 96-well plate so that there were 3000 cells in each well. The plates were incubated for 24 h in an incubator (Germany, Memmert) to return the cells to normal from the stress of trypsinization. Then, suitable dilutions of the desired Fe_3O_4, $Cu(NO_3)_2$, and Fe_3O_4-NH_2@CS/CuO nanocomposite were prepared and 100 µl of each dilution was added columnar to the plate wells and the cells were incubated for 37 h at 37 °C and 5% CO_2. After 72 h of adding the Fe_3O_4, $Cu(NO_3)_2$, and Fe_3O_4-NH_2@CS/CuO nanocomposite to the cells, 20 µl of 5 mg/ml MTT solution was added to each well. The plates were incubated for 4 h after the required time, the culture medium containing MTT was carefully removed and 100 µl of DMSO was added to each well to dissolve the resulting formazan. After 10 min and shaking the plates using the plate shaker, the light absorption at 570 nm was read by ELISA Reader (Awareness Technology Inc, Stat Fax 2100, USA). Cells containing no Fe_3O_4, $Cu(NO_3)_2$, and Fe_3O_4-NH_2@CS/CuO nanocomposite were considered as controlled light density and wells without cells and only RPMI1640 medium with bovine fetal serum were considered as blank (Lu et al., 2021).

$$\text{Cell viability}(\%) = \frac{\text{Sample A.}}{\textit{Control A.}} \times 100$$

Finally, linear regression was performed to obtain the IC50 level, which represents the concentration of the extract, which causes 50% inhibition of cancer cell growth (Lu et al., 2021):

3. Results and discussion

3.1. Analysis of catalytic characterization data

The method of FT-IR spectroscopy is used for detecting unknown substances, determining the quality or uniformity of the sample, determining the amount of ingredients in a mixture, identify mixtures of organic and inorganic compounds provided they are both solid or liquid, thin layer analysis, analysis of adhesives, coatings and adhesive enhancers or binders, identification of polymers and polymer mixtures, analysis of solvents, cleaners and detergents unknown, percentage of decomposition or non-polymerization of polymers and paints due to heat, UV or other factors, determination of the degree of crystallization in polymers, and analysis of resins, composite materials and metal nanoparticles (Lotfi and Veisi, 2019; Lu et al., 2021; Rathore et al., 2014).

FT-IR spectra of the Fe_3O_4, Fe_3O_4-NH_2, CS, Fe_3O_4-NH_2@CS and Fe_3O_4-NH_2@CS/CuO are shown in Fig. 1 to confirm the successful synthesis of desired nanocomposite. Fig. 1a presents the representative peaks of bare Fe_3O_4 NPs, where the sharp bands at 582–637 cm^{-1} correspond to Fe–O–Fe stretching vibrations. Fig. 1b shows a broad band at 3000–3500 cm^{-1} attributing to OH and NH_2 stretching vibrations. A strong band at 550–650 cm^{-1} indicates the presence of Fe-O bond. The broadband at 1100 cm^{-1} can be assigned to Si-O-Si bond stretching vibration. The sp^3 C-H stretching and NH_2 bending vibrations appear at around 2800 and 1550 cm^{-1} respectively, indicating the aminopropyl attachment with the ferrite surface. FT-IR spectra of chitosan (Fig. 1c) shows a broad peak at 3429 cm^{-1} corresponding to the overlapped stretching vibrations of NH_2 and OH groups. The alcoholic C–O stretching, asymmetric C–O–C (glycosidic) stretching, C–N stretching and N–H bending peaks are observed at 1380 cm^{-1}, 1156 cm^{-1}, 1027 cm^{-1} and 1590 cm^{-1} respectively. Fig. 1d shows the IR absorptions for Fe_3O_4-NH_2@CS material. It represents all the individual peaks from Fe_3O_4, silica layers, and chitosan indicating successful assembling. Only, the corresponding peaks are seen to be slightly moved to higher or lower regions. An additional peak is observed at 1635 cm^{-1}, attributed to the imine functionality (C═NH) formed during intermolecular cross-linking. Finally, in the analysis of Fe_3O_4-NH_2@CS/CuO nanocomposite we observed almost the same fashion as Fig. 1d except for very slight peak shifts of the imine, alcoholic C–O, C–N stretching vibrations to 1625, 1431, 1046 cm^{-1} due to strong complexation of the corresponding functions to the Cu(II) NPs. The Fe-O bond vibration was also found moved to 564 cm^{-1}.

Today, FE-SEM is used not only in materials science, chemistry and physics, but also in many fields such as medical and biological sciences. The high resolution of FE-SEM makes it one of the most-powerful and comprehensive tools for examining and analyzing a wide range of microstructure characteristics of samples at the nanometer to micrometer scale. Using the above technique, we can determine how the particles are placed from each other, their morphology and size (Shaib et al., 2013; Raut et al., 2010).

The morphological structure of the Fe_3O_4-NH_2@CS/CuO nanocomposite were studied by FE-SEM and TEM analysis. The globular shape nanoparticles can be detected from the FE-SEM image having a mean diameter of ~20–30 nm (Fig. 2). The surface modification over Fe_3O_4 NPs by CS polymers can be adjudged from its appearances. There occurs a homogeneous growth of chitosan over it.

EDX is a method that uses X-ray energy to analyze the structure and chemical composition of samples on a small scale. Using the EDX analysis method, qualitative and quantitative analysis can be performed on a wide range of metallurgical, biological, mineral and ceramic samples. Using the obtained information, it is possible to investigate the quantity and quality of specific phases and areas with homogeneous chemical composition. In other words, this method can be used for microanalysis (Shaib et al., 2013; Raut et al., 2010). In EDX analysis, by measuring the energy of the emitted rays, we can identify the type of element under study, which is a method of qualitative analysis. By measuring the intensity of

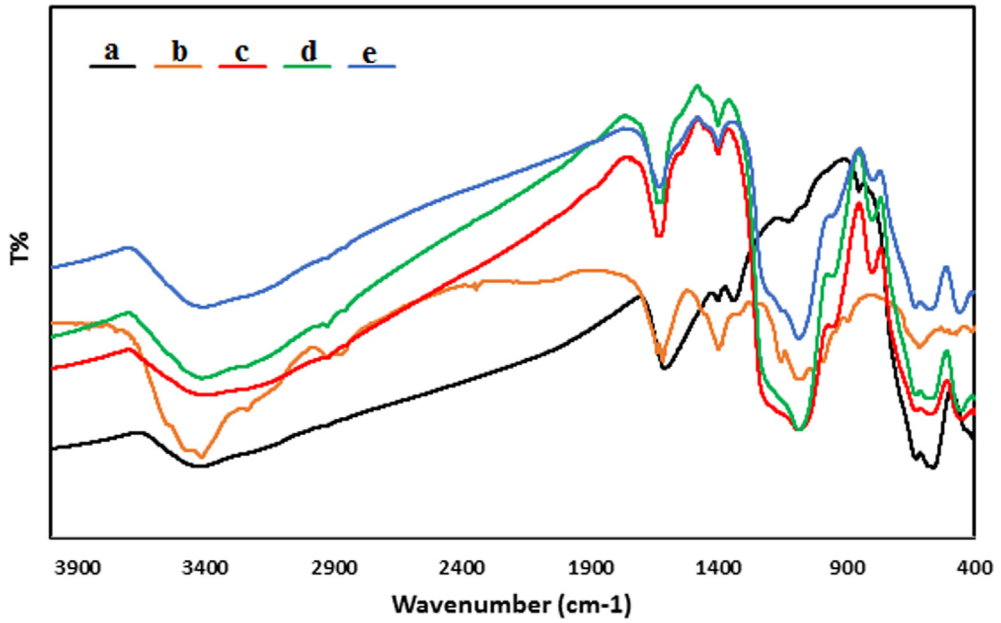

Fig. 1 FT-IR spectra of a) Fe_3O_4, b) Fe_3O_4-NH_2, c) CS, d) Fe_3O_4-NH_2@CS and e) Fe_3O_4-NH_2@CS/CuO nanocomposite.

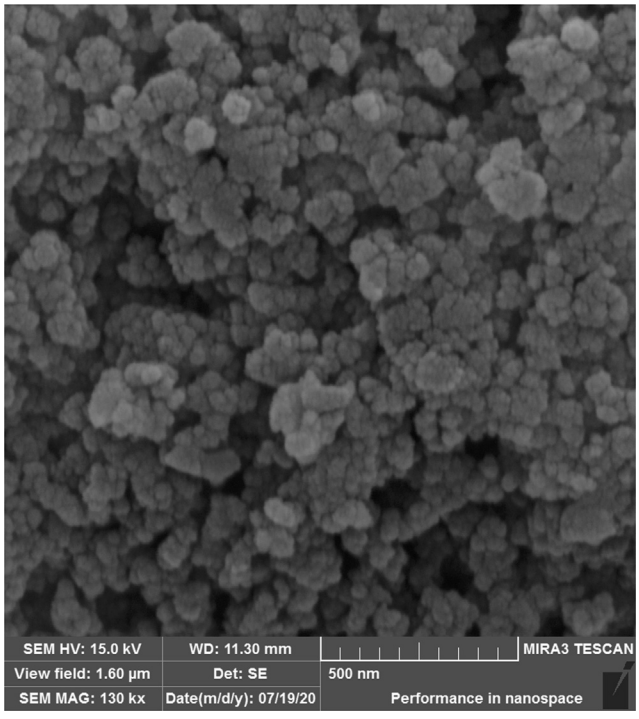

Fig. 2 FESEM image of Fe_3O_4-NH_2@CS/CuO nanocomposite.

X-rays, the concentration of sample elements can be determined, making it possible to quantitatively analyze unknown samples. The higher the observed ipak for the element in the graph, the higher the concentration of that element in the sample. Also, as the energy of the electron beam increases and the atomic weight of the elements decreases, more depth can be obtained from the sample information (Lotfi and Veisi, 2019; Lu et al., 2021).

EDX analysis of the Fe_3O_4-NH_2@CS/CuO nanocomposite exhibits Fe, Si, C, N, O and Cu species (Fig. 3). It confirmed the successful preparation of the desired nanocomposite. C and N atoms came from chitosan that coated on the surface of Fe_3O_4 nanoparticles.

The data obtained from EDX analysis were further rationalized through elemental mapping. X-ray scanning of a section of FESEM image reveals the uniform distribution of Fe, Si, C, N, O and Cu atoms over the nanocomposite surface (Fig. 4).

One of the things that play a key role in the study of nanoparticles is determining their size. Transmission Electron Microscopy (TEM) is one of the most effective methods in determining particle size, which can provide us with useful quantitative and qualitative information. The TEM test is a method that allows direct imaging of particles up to the size of an atom, and this advantage of direct imaging must be considered when working with a microscope. Appropriate qualitative analysis of nanoparticles requires optimization of different imaging methods, magnification and manual or automatic analysis methods whose purpose is to optimize the image sharpness and contrast between the sample particles and the appropriate number of particles in each image, while minimizing damage to the sample. At lower image magnifications, it is possible to study the particle distribution, however, at high magnifications, a large number of particles are not observed and only information about the orientation of the plates and the structure is provided. In addition, at high magnification, high electron current causes instability and damage to the structure under study (Shaib et al., 2013; Raut et al., 2010; Lotfi and Veisi, 2019; Lu et al., 2021). The particle size distribution histograms for Fe_3O_4, Fe_3O_4-NH_2 and Fe_3O_4-NH_2@CS whose average size are approximately 15.8, 24.3 and 25.4 nm respectively (Fig. 5). This results confirmed the successful modification of materials for final composite.

TEM study of the nanocomposite is presented in Fig. 5. The thin layer of chitosan bio-polymer surrounding the black

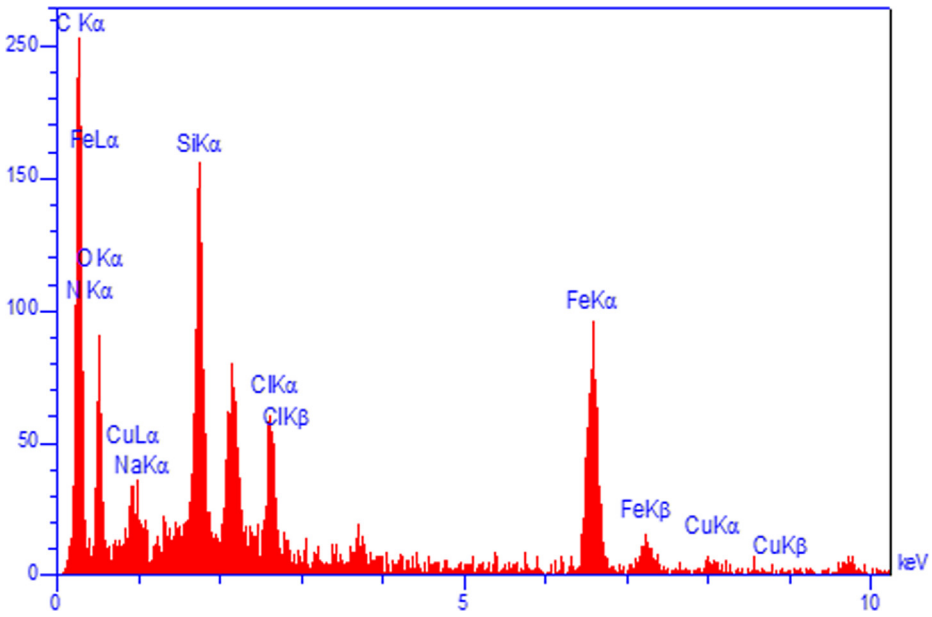

Fig. 3 EDX pattern of Fe_3O_4-NH_2@CS/CuO nanocomposite.

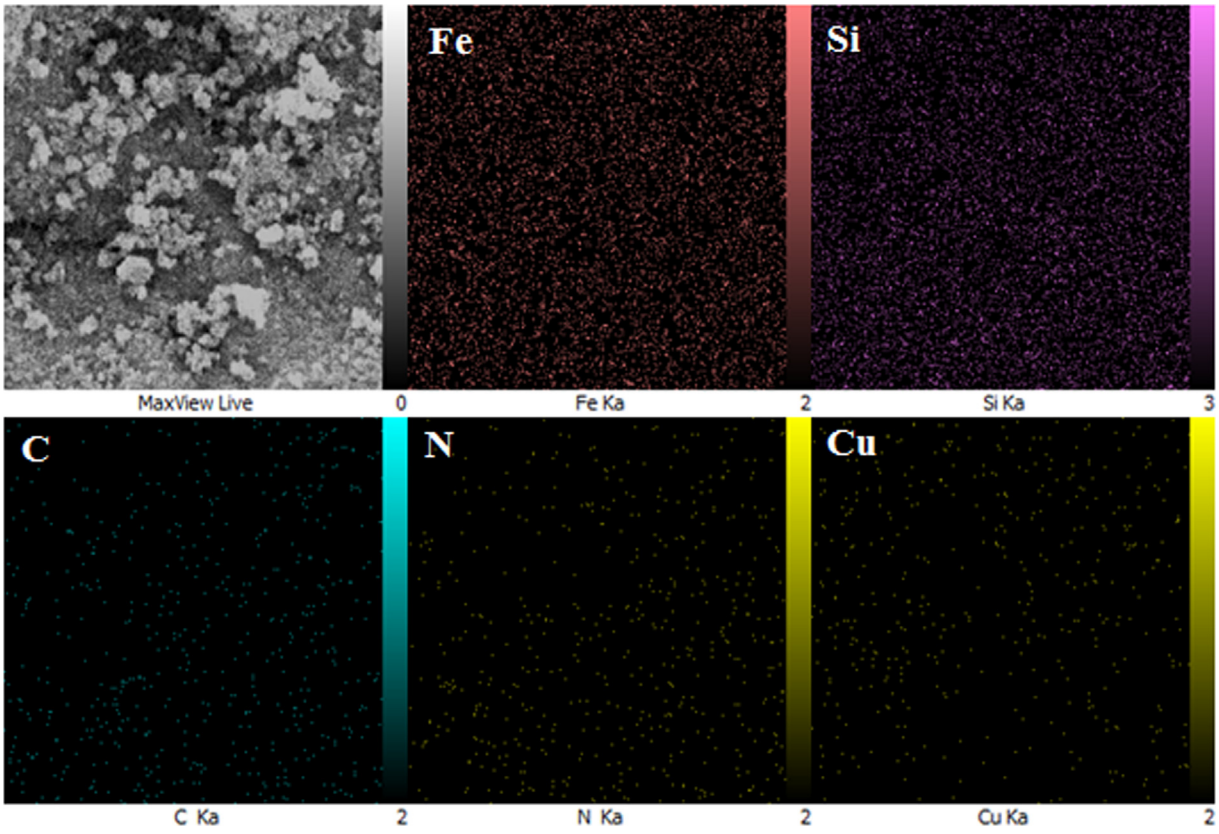

Fig. 4 Elemental mapping of Fe_3O_4-NH_2@CS/CuO nanocomposite, Fe, Si, C, N and Cu respectively.

colored Fe_3O_4 NPs can be detectable. The size of the final nanocomposite particles was in accordance with SEM study and is around ~20–30 nm. The tiny black dots correspond to the Fe_3O_4 NPs. These data demonstrate the proposed architecture of the material. Moreover, Fig. 6 (inset) determines the particle size distribution histograms for Fe_3O_4-NH_2@CS/CuO nanocomposite whose average size are approximately 27.6 nm.

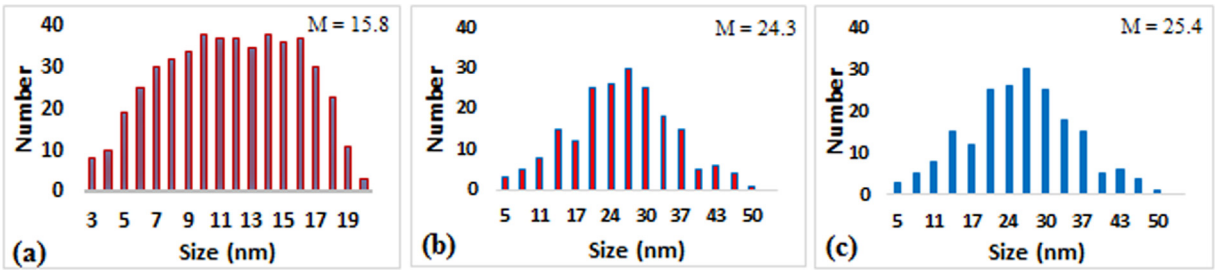

Fig. 5 The particle size distribution histograms for (a) Fe_3O_4, (b) Fe_3O_4-NH_2 and (c) Fe_3O_4-NH_2@CS.

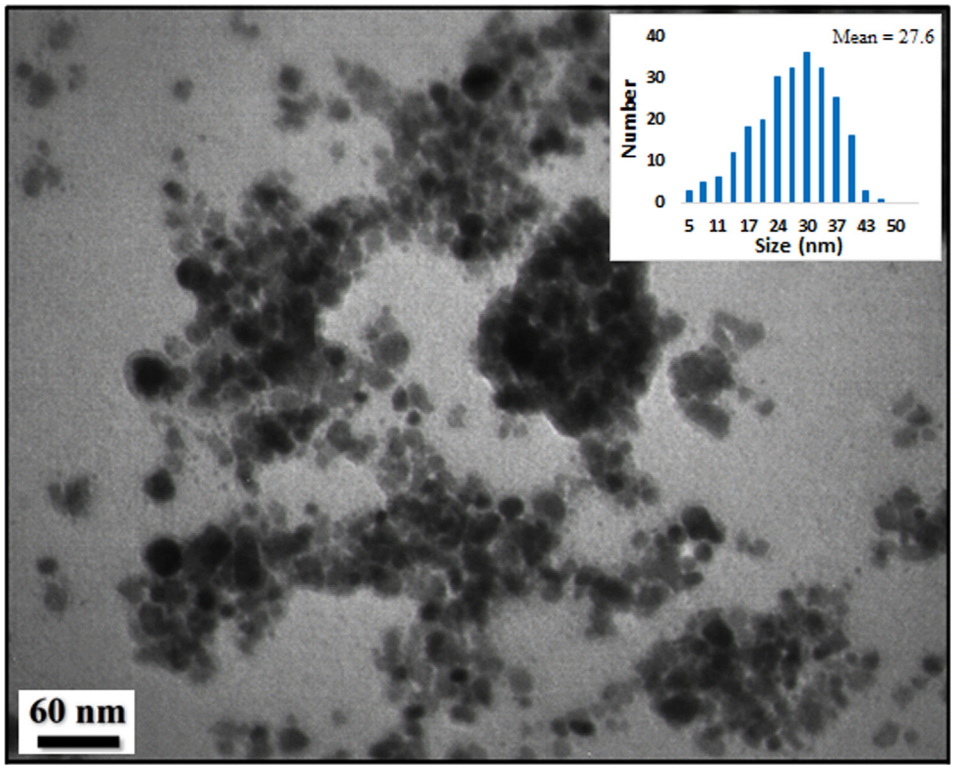

Fig. 6 TEM images of Fe_3O_4-NH_2@CS/CuO nanocomposite and its particle size distribution histogram (inset).

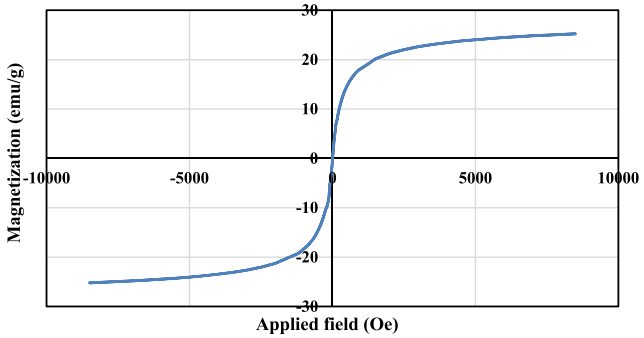

Fig. 7 VSM analysis of Fe_3O_4-NH_2@CS/CuO nanocomposite.

The saturation magnetization (*M*s) value obtained from magnetic hysteresis loops of Fe_3O_4-NH_2@CS/CuO nanocomposite was 25.22 emu/g (Fig. 7). Still, the desired nanocomposite behaves like a superparamagnetic and can be easily isolated by an external magnet.

3.2. Anti-human gastro-duodenal cancers properties of Cu $(NO_3)_2$, Fe_3O_4, and Fe_3O_4-NH_2@CS/CuO nanocomposite

Despite many advances in disease control and treatment, cancer remains one of the global challenges to human health. The most common treatment for cancer is chemotherapy. An important point in the treatment of cancer with chemotherapy is the acquired resistance of the tumor to drugs, and this has created major problems for the treatment of cancer (Juul et al., 2018; Lauby-Secretan et al., 2016; Cunningham et al., 2010). Because the rate of mutation and genetic instability in cancer cells is very high and genetic changes occur rapidly in them, these cells become resistant to drugs. Therefore, further research on discovering new treatment strategies to overcome the drug resistance of cancers seems necessary (Shaib et al., 2013; Raut et al., 2010). Meanwhile, nanotechnology has created a promising field in cancer treatment. Recently, the anti-cancer and anti-angiogenic effects of metallic nanoparticles have been considered and the results have shown that

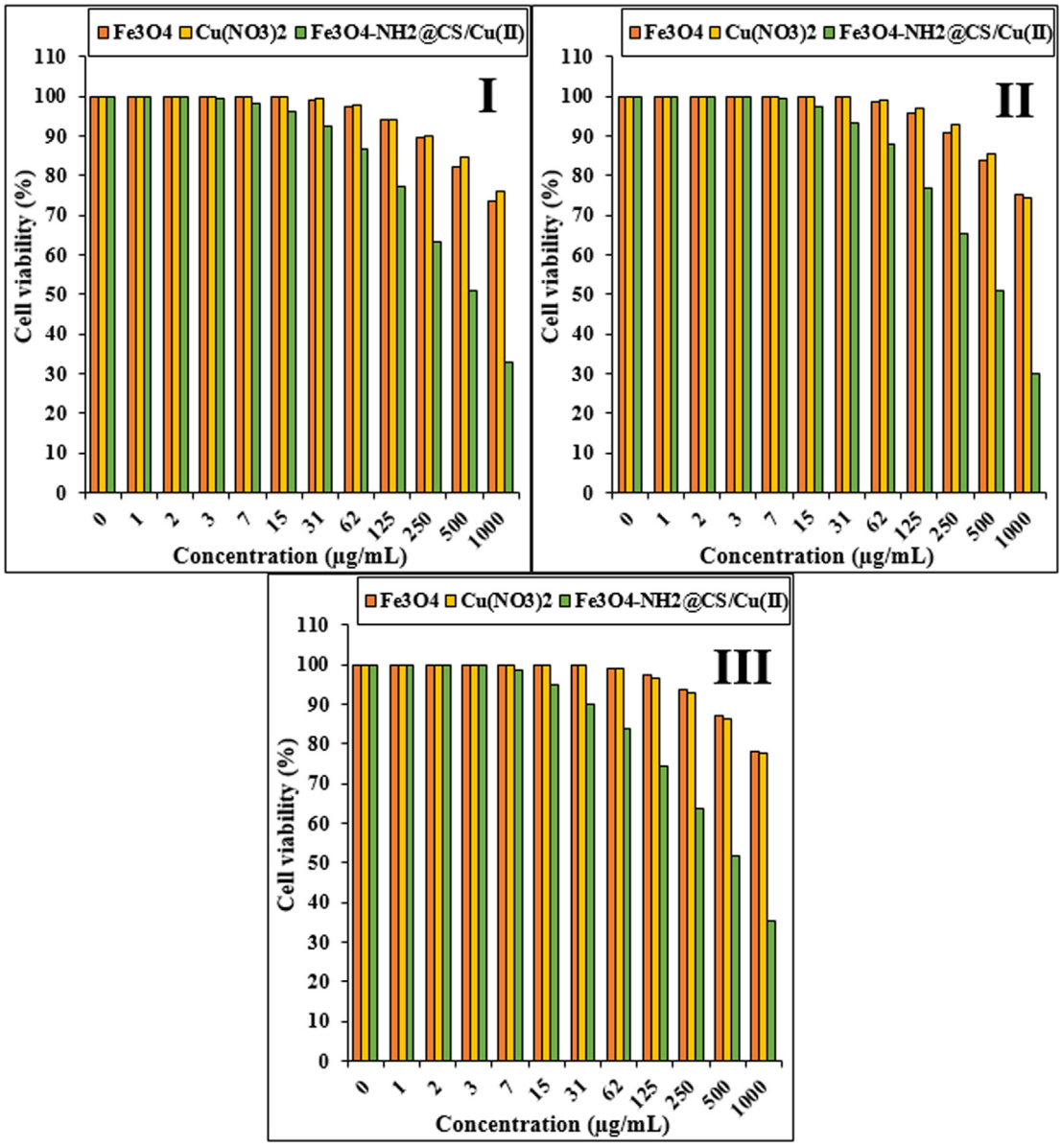

Fig. 8 The anti-gastric cancer properties of Fe_3O_4, $Cu(NO_3)_2$, and Fe_3O_4-NH_2@CS/CuO nanocomposite against MKN45 (A), AGS (B), and KATO III (C) cell lines.

metallic nanoparticles can be considered as a potential anticancer agent (Shaib et al., 2013; Raut et al., 2010; Lotfi and Veisi, 2019; Lu et al., 2021).

Many parameters such as surface functions nature and texture and size are important in the anticancer effects of metallic nanoparticles, of course the efficacy of the size is the main (Lotfi and Veisi, 2019). Many reports have been indicated whatever the nanoparticles size is low, their ability in poring and destroying the cancer cells is more. In detail, it has been reported the nanoparticles with the size lower than 50 nm have the best condition for anticancer effects (Lotfi and Veisi, 2019; Lu et al., 2021). As shown in the TEM images, the size of nanoparticles is less than 30 nm.

In the current experiment, the cytotoxicity of $Cu(NO_3)_2$, Fe_3O_4, and Fe_3O_4-NH_2@CS/CuO nanocomposite was explored by examining its interaction with human gastric cancer cell lines i.e. MKN45, AGS, and KATO III and human colorectal carcinoma cell lines.

The interactions being expressed as cell viability (%) was seen at several $Cu(NO_3)_2$, Fe_3O_4, and Fe_3O_4-NH_2@CS/CuO nanocomposite concentrations (0–1000 µg/mL) with the eight-cell lines which have been indicated in Figs. 8–10. In all the cases, the % cell viability gets decreased with raising $Cu(NO_3)_2$, Fe_3O_4, and Fe_3O_4-NH_2@CS/CuO nanocomposite samples concentrations. The IC50 of Fe_3O_4-NH_2@CS/CuO nanocomposite against MKN45, AGS, KATO III, HT-29, HCT 116, HCT-8 [HRT-18], and Ramos.2G6.4C10 cell lines were 517, 525, 544, 282, 214, 420, and 477 µg/mL, respectively (Tables 1 and 2). Thereby, the best anti-gastro-duodenal cancers findings of our Fe_3O_4-NH_2@CS/CuO nanocomposite was observed in the case of the HCT 116 cell line (Table 2).

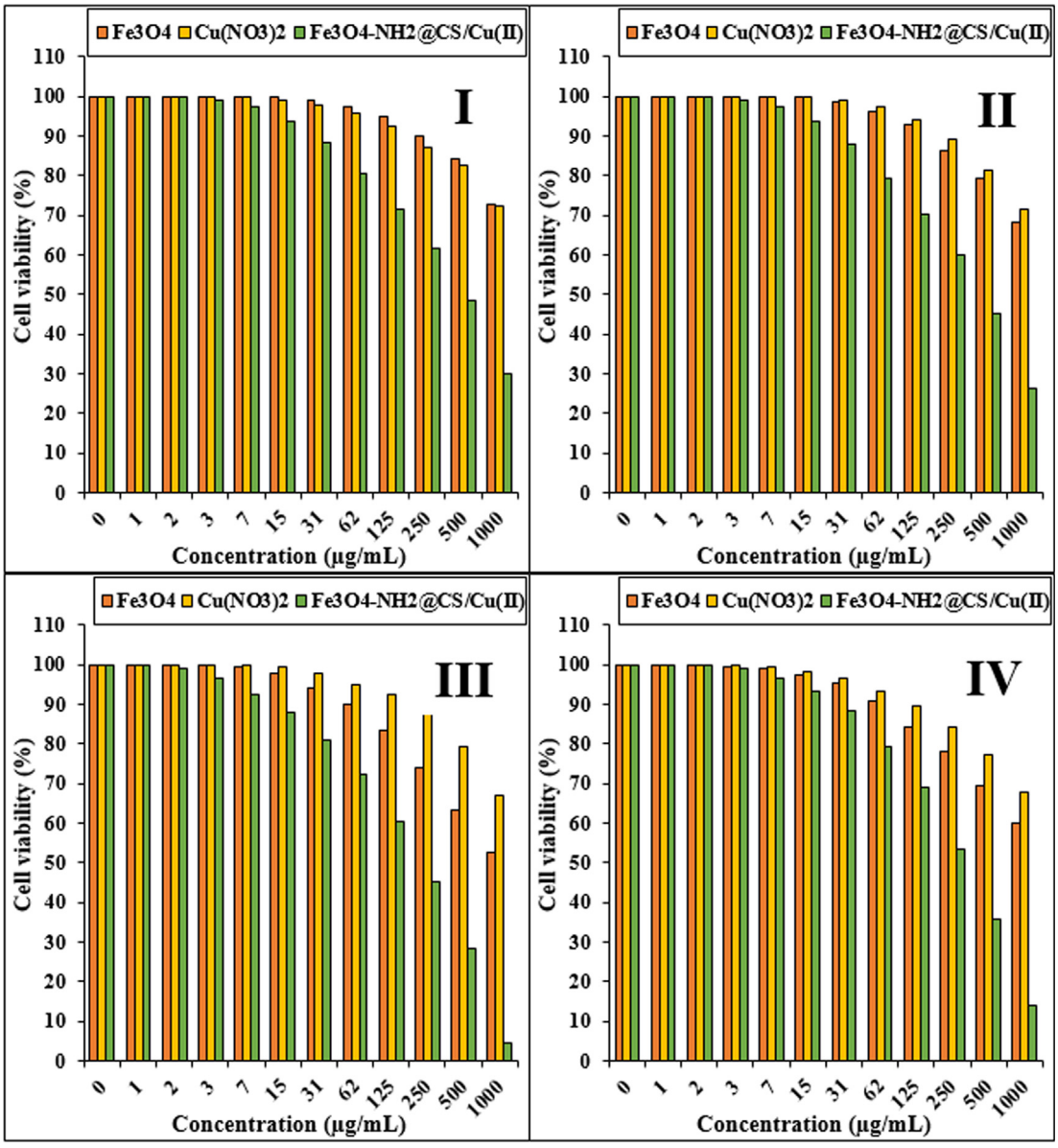

Fig. 9 The anti-colorectal carcinoma properties of Fe_3O_4, $Cu(NO_3)_2$, and Fe_3O_4-NH_2@CS/CuO nanocomposite against Ramos.2G6.4C10 (I), HCT-8 [HRT-18] (II), HCT 116 (III), and HT-29 (IV) cell lines.

Oxidation from reactive oxygen species can cause cell membrane disintegration, damage to membrane proteins, and DNA mutation that the result is the onset or exacerbation of many diseases (Shaib et al., 2013; Raut et al., 2010; Soni and Krishnamurthy, 2013; Katata-Seru et al., 2018; Sangami and Manu, 2017). Antioxidants with the property of removing free radicals play an important role in the prevention or treatment of oxidation-related diseases or free radicals. Extensive molecular cell research on cancer cells has developed a targeted approach to the biochemical prevention of cancers that the goal is to stop or return cells to their pre-cancerous state without any toxic doses through nutrients and drugs. Numerous studies have been performed on the use of natural compounds as anti-cancer agents in relation to appropriate antioxidant activity (Shaib et al., 2013; Raut et al., 2010; Lotfi and Veisi, 2019; Lu et al., 2021; Soni and Krishnamurthy, 2013; Katata-Seru et al., 2018; Sangami and Manu, 2017; Beheshtkhoo and Kouhbanani, 2018; Radini et al., 2018).

It seems the high anti-human gastro-duodenal cancers properties of Fe_3O_4-NH_2@CS/CuO nanocomposite are related to its antioxidant activities. Our successful efforts to utilize Fe_3O_4-NH_2@CS/CuO nanocomposite in gastro-duodenal cancers studies certainly shed light on future studies in this area.

4. Conclusions

In conclusion, we described the preparation of Fe_3O_4-NH_2@CS/CuO nanocomposite by coordinating Cu(II) NPs over chitosan functionalized Fe_3O_4 nanoparticles. The material was characterized by FT-IR spectroscopy, FE-SEM, TEM XRD, VSM and EDX analysis. In the oncological part

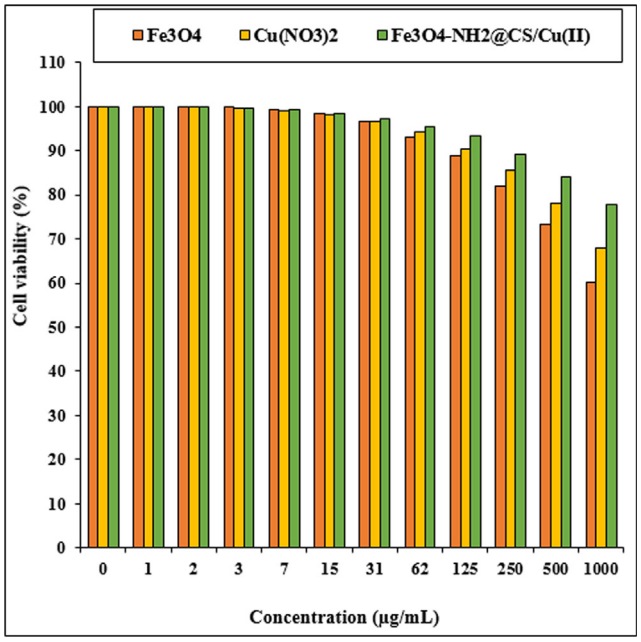

Fig. 10 The cytotoxicity effects of Fe_3O_4, $Cu(NO_3)_2$, and Fe_3O_4-NH_2@CS/CuO nanocomposite against Normal (HUVEC) cell line.

Table 1 The IC50 of Fe_3O_4, $Cu(NO_3)_2$, and Fe_3O_4-NH_2@CS/CuO nanocomposite in the anti-gastric cancer test.

	Fe_3O_4 (µg/mL)	$Cu(NO_3)_2$ (µg/mL)	Fe_3O_4-NH_2@CS/CuO (µg/mL)
IC50 against MKN45	–	–	517 ± 0[a]
IC50 against AGS	–	–	525 ± 0[a]
IC50 against KATO III	–	–	544 ± 0[a]
IC50 against HUVEC	–	–	–

Table 2 The IC50 of Fe_3O_4, $Cu(NO_3)_2$, and Fe_3O_4-NH_2@CS/CuO nanocomposite in the anti-colorectal carcinoma test.

	Fe_3O_4 (µg/mL)	Cu $(NO_3)_2$ (µg/mL)	Fe_3O_4-NH_2@CS/CuO (µg/mL)
IC50 against Ramos.2G6.4C10	–	–	477 ± 0[b]
IC50 against HCT-8 [HRT-18]	–	–	420 ± 0[b]
IC50 against HCT 116	–	–	214 ± 0[a]
IC50 against HT-29	–	–	282 ± 0[a]
IC50 against HUVEC	–	–	–

of the present study, the cell viability of Fe_3O_4, $Cu(NO_3)_2$, and Fe_3O_4-NH_2@CS/CuO nanocomposite was determined against human gastric cancer cell lines i.e. MKN45, AGS, and KATO III and human colorectal carcinoma cell lines by MTT assay for 48 h. It indicated notable cytotoxicity, anti-human gastric cancer, and anti-human colorectal carcinoma effects of Fe_3O_4-NH_2@CS/CuO nanocomposite in the *in vitro* condition. It looks the resent nanocomposite may be administrated to cure gastro-duodenal cancers in the near future.

5. Ethics explanation

This research was approved by Yijishan Hospital of Wannan Medical College animal ethical committee, Approved No. YJSH2100430.

Declaration of Competing Interest

The authors declare that they have no known competing financial interests or personal relationships that could have appeared to influence the work reported in this paper.

Acknowledgments

The authors extend their appreciation to the deanship of Scientific Research at King Khalid University, Abha, Saudi Arabia, for supporting this work under grant number (R.G. P.2/122/42), and the work was supported by the Taif University Researchers Supporting Project Number (TURSP-2020/99), Taif University, Taif, Saudi Arabia.

References

Astin, M., Griffin, T., Neal, R.D., Rose, P., Hamilton, W., 2011. The diagnostic value of symptoms for colorectal cancer in primary care: a systematic review. Br. J. Gen. Pract. 61, 231–243.
Beheshtkhoo, N., Kouhbanani, M.A.J., Savardashtaki, A., 2018. Appl. Phys. A 124, 363–369.
Cunningham, D., Atkin, W., Lenz, H.J., Lynch, H.T., Minsky, B., Nordlinger, B., Starling, N., 2010. Colorectal cancer. Lancet. 375, 1030–1047.
Juul, J.S., Hornung, N., Andersen, B., Laurberg, S., Olesen, F., Vedsted, B., 2018. The value of using the faecal immunochemical test in general practice on patients presenting with non-alarm symptoms of colorectal cancer. Br. J. Cancer. 119, 471–479.
Katata-Seru, L., Moremedi, T., Aremu, O.S., 2018. J. Mol. Liq. 256, 296–304.
Lauby-Secretan, B., Scoccianti, C., Loomis, D., Grosse, Y., Bianchini, F., Straif, K., 2016. Body Fatness and Cancer– Viewpoint of the IARC Working Group. N. Engl. J. Med. 375, 794–798.
Lotfi, S., Veisi, H., 2019. Mat. Sci. Eng. C 105, 110112.
Lu, Y., Wan, X., Li, L., Sun, P., Liu, G., 2021. Synthesis of a reusable composite of graphene and silver nanoparticles for catalytic reduction of 4- nitrophenol and performance as anti-colorectal carcinoma. J. Mater. Res. Technol. 12, 1832–1843.
Radini, I.A., Hasan, N., Malik, M.A., 2018. J. Photochem. Photobiol. B 183, 154–163.
Rathore, P.S., Patidar, R., Thakore, S., 2014. RSC Adv. 4, 41111.
Raut, R.W., Kolekar, N.S., Lakkakula, J.R., Mendhulkar, V.D., Kashid, S.B., 2010. Nano-Micro Lett. 2, 106–113.
Sangami, S., Manu, M., 2017. Environ. Technol. Innov. 8, 150–163.
Shaib, W., Mahajan, R., El-Rayes, B., 2013. Markers of resistance to anti-EGFR therapy in colorectal cancer. J. Gastrointest. Oncol. 4, 308–318.
Soni, A., Krishnamurthy, R., 2013. Indian J. Plant. Sci. 2, 117–125.